ELSEVIER

Journal of Chromatography A, 737 (1996) 181–192

JOURNAL OF CHROMATOGRAPHY A

Application of radio-chromatographic techniques to diesel emissions research

P.J. Tancell*, M.M. Rhead

Department of Environmental Sciences, University of Plymouth, Devon, PL4 8AA, UK

Received 27 October 1995; revised 9 January 1996; accepted 9 January 1996

Abstract

The development of radio-high-performance liquid chromatographic (radio-HPLC) techniques and radio-gas chromatographic (radio-GC) techniques and their application to the field of diesel emission research is described. These techniques have been used to investigate the emission of organic components and specifically polycyclic aromatic hydrocarbons (PAHs) in diesel exhaust. In a series of experiments radiolabelled [^{14}C]PAH tracers were combusted in a 2-l direct injection Perkins Prima diesel engine. Exhaust emissions were sampled using an exhaust gas sampling system, the total exhaust solvent scrubbing apparatus. Radioactive products of combustion in the exhaust emissions were identified and quantified using both radio-GC and radio-HPLC. The benefits and limitations of each technique are discussed in the context of diesel emissions research.

Keywords: Radiochromatography; Diesel exhaust; Environmental analysis; Air analysis; Polynuclear aromatic hydrocarbons

1. Introduction

Diesel exhaust emissions are of concern owing to their adverse effects on human health, especially in the urban environment [1,2]. Of particular concern are the polycyclic aromatic hydrocarbons (PAHs) which are emitted in diesel exhaust as a gaseous phase or adsorbed to fine particulate material. Certain PAHs have been classified by the International Agency for Research on Cancer (IARC) as probable human carcinogens [2]. Diesel passenger cars are a significant contributor to the atmospheric burden of PAHs in urban areas [1] and the increase in their sales observed in recent years is set to continue [3].

This research programme has investigated the origin of organic species and especially PAHs in diesel emissions using ^{14}C-radiolabelled precursors. The application of ^{14}C-radiolabelling techniques to the field of diesel emissions research is unique to this research group and yields information that is difficult to obtain using other techniques. The primary advantages associated with the use of radiotracers in this research are the ability to identify unambiguously the origin of organic species in the emissions and the ability to quantify their contribution [4]. Determining the origin of these species in diesel exhaust is essential if control strategies aimed at reducing their emissions are to be effective.

The use of ^{14}C-labelled radiotracers has necessitated the development of sophisticated methods of analysis for the identification and quantification of radioactive products of combustion in the exhaust emissions. This paper reports on the development of two radio-chromatographic techniques, radio-high-

*Corresponding author.

0021-9673/96/$15.00 © 1996 Elsevier Science B.V. All rights reserved
PII S0021-9673(96)00040-4

performance liquid chromatography (radio-HPLC) and radio-gas chromatography (radio-GC) and their application to the analysis of the organic fraction of diesel exhaust emissions. The benefits and limitations of each technique are discussed with respect to this area of research. The optimization of the two systems is explained and examples of the analysis of exhaust samples originating from the combustion of ^{14}C-labelled fuel components are presented.

2. Experimental

2.1. Reagents

[1,4,5,8-^{14}C]Naphthalene, [7,10-^{14}C]benzo[*a*]pyrene [B(*a*)P] and [1-^{14}C]hexadecane were purchased from Amersham International, UK. [9-^{14}C]Fluorene and [8-^{14}C]2-methylnaphthalene were obtained from Sigma, USA. The stated radiochemical purity was ≥98% for all PAHs. Non-labelled PAH standards were purchased from Aldrich, UK. All solvents were of HPLC grade (Rathburns) and were used as received.

2.2. Exhaust sampling and preparation

Exhaust samples were collected using the total exhaust solvent stripping apparatus (TESSA) [5]. Exhaust samples were collected in approximately 2 l of dichloromethane–methanol and were isolated and concentrated according to the method described previously [6]. The total exhaust sample (TES) was separated into aliphatic, aromatic and polar fractions by silica open-column chromatography [6]. The aromatic fraction was further separated according to ring size by normal-phase preparative HPLC using an amino-bonded silica-gel column with simultaneous radio-detection [4]. This fractionation yielded five subsamples; benzenes (1-ring), naphthalenes (2-rings), fluorenes and dibenzothiophenes (3-rings), phenanthrenes (3-rings) and a fraction containing PAHs with 4 and 5 fused rings. Aliphatic and aromatic subsamples were analysed by radio-HPLC and radio-GC.

2.3. Radio-HPLC

The HPLC system comprised dual pumps (Merck-Hitachi L-6200A intelligent pump and L-6000 LC pump) with UV–Vis and fluorescence spectrophotometers (Merck-Hitachi L-4200 and Merck-Hitachi F-1050, respectively) connected in series. Separations were performed on a Supelcosil LC-PAH column (250 × 4.6 mm I.D., Supelco) packed with 5-μm polymeric octadecyl-bonded silica and using an acetonitrile–water mobile phase. A solvent gradient was employed to optimize the separation of sample components and was varied for the individual exhaust subsamples. For the analysis of the naphthalene, fluorene and phenanthrene subsamples of diesel exhaust, the solvent gradient employed an initial solvent composition of acetonitrile–water (60:40) held isocratically (5 min) and changed linearly to 100% acetonitrile over 20 min and held for 20 min. In the analysis of the exhaust subsample containing 4- and 5-ring PAHs the initial composition of the mobile phase was acetonitrile–water (80:20) which was raised linearly to 100% acetonitrile over 10 min followed by 100% acetonitrile for 20 min. The flow-rate was 1 ml/min in all analysis. Detection of the 4- and 5-ring aromatic subsample was by fluorescence. Excitation (λ_{ex}) and emission (λ_{em}) wavelengths were selected to improve the sensitivity and selectivity of detection for individual PAHs [7]. For the analysis of B(*a*)P wavelengths of λ_{em} = 430 nm and λ_{ex} = 365 nm were chosen. Detection for the other fractions was by UV absorption at 254 nm.

Radioactivity measurement was performed using a Berthold LB 506 C-1 detector linked to UV–Vis and fluorescence detectors in series. The monitor was equipped with a yttrium glass solid scintillant measuring cell (0.15 ml cell volume). Noise and luminescence events were detected and compensated for using a coincidence circuit with a resolution time of 100 ns. Radioactivity data collection was performed using a Berthold radio-HPLC software package.

2.4. Radio-GC

The radio-GC system comprised a Varian 3400 gas chromatograph and a Lablogic radioactivity monitoring (RAM) system. The gas chromatograph was equipped with a flame ionization detection (FID) system and temperature programmed on-column injection with cryogenic cooling. The detector temperature was maintained at 320°C. The injector

temperature program employed an initial injector temperature of −20°C raised to 250°C at 250°C/min. All samples were dissolved in dichloromethane. The GC system was fitted with a DB-5, megabore column (30 m × 0.53 mm I.D., 0.25 μm film thickness, J & W Scientific). Deactivated fused-silica tubing (2 m × 0.32 mm I.D.) was installed between the injector and the column as a retention gap. Helium was used as carrier gas at a velocity of 42 cm/s for optimum separation efficiency [8]. A mass flow controller was used to ensure a constant flow-rate. Separations were performed using a temperature gradient employing an initial temperature of 40°C raised linearly to 300°C at 5°C/min and held for 20 min.

The effluent from the column was divided using a variable outlet splitter system (SGE, OSS-2). The splitter contains a needle valve which allows the split ratio to be varied over a wide range (up to 1000:1). The detector requiring the least proportion of the eluent (in our case the FID system) is connected to the base of the splitter. The flow to this detector can be stopped as required (for instance in the calculation of counting efficiencies) by closing the valve. Helium make-up gas was added to the column eluent, at a flow of ≈25 ml/min, prior to the eluent split through a tee-piece incorporated in the needle valve. Connections for supply of the make-up gas were 1.6 mm I.D. stainless-steel tubing. Addition of make-up gas at this point in the system helps eliminate problems of dead volume. Deactivated silica capillary tubing (50 cm × 0.32 mm I.D.) connected the two outlets from the splitter with the FID system and radioactivity detectors.

Radioactivity measurement was performed using a flow through gas proportional counting tube. The counting tube contained a highly polished stainless-steel outer tube and a gold-plated tungsten (0.005 mm O.D.) anode wire and has been constructed so as to ensure laminar gas flow through its volume in order to minimize turbulent gas mixing. Two mass flow sensors measure the scintillant gas flow entering the counting tube and the total gas flow exiting the tube. An oxidation furnace, containing copper oxide catalyst, oxidized ^{14}C-radiolabelled sample components to $^{14}CO_2$ prior to mixing with the scintillant gas. The furnace was situated inside the GC oven to avoid condensation of sample components in the deactivated silica tubing connecting the furnace and column. The furnace temperature, measured using a thermocouple, was maintained at 700°C. The external temperature of the furnace was 80°C. The furnace is connected to a drying tube (100 × 0.3 mm I.D.) filled with granular anhydrous sodium sulphate by 1.6 mm I.D. stainless-steel tubing. The drying tube removed water vapour from the furnace eluent which would otherwise quench the signal in the counting tube. Scintillant gas (argon–methane, 90:10) was added to the effluent mixture prior to the counting tube. The detector was remotely controlled from a PC using a Windows-based software package (Lablogic Laura, Ver. 1.1, radio-chromatography software) which enabled simultaneous data collection from the mass and radioactivity detectors.

3. Results and discussion

Diesel exhaust is a highly complex matrix containing many hundreds of individual species [9]. Pre-fractionation steps are routinely employed to reduce their complexity and to facilitate component identification [10]. This is especially the case where component identification must be made using retention index data alone and was essential in the current research owing to the lack of a specific detector in combination with radio-GC or radio-HPLC. The fractionation procedure employed a primary clean-up and separation by silica column chromatography followed by a second fractionation using normal-phase semi-preparative HPLC. The reduced number of components in individual subsamples has facilitated component identification in the subsequent analytical procedures. The fractionation procedure has the added advantage of increasing the specific activity of the radioactive components in the exhaust subsamples thereby ensuring that sufficient radioactivity was present to be above the limit of detection of the radio-GC and radio-HPLC analyses.

3.1. Compromise between radio-detector sensitivity and chromatographic resolution

One of the main goals in developing both the radio-GC and radio-HPLC systems was the need to retain chromatographic performance, which is essential to component identification, whilst maximizing

Table 1
Effect of total gas flow-rate on peak width and detector sensitivity in radio-GC

Total flow (ml/min)	w_{FID} (s)	w_{RAD} (s)	Residence time (s)	[1-^{14}C]*n*-Hexadecane radio-peak integral
60	9.4	23.1	10	1920
130	8.8	16.9	4.6	510

the sensitivity of the radio-detectors. In flow-through radioactivity monitors, resolution and sensitivity are interdependent and any improvement in one is gained at the expense of the other. The compromise between sensitivity and resolution is primarily a function of the eluent flow through the radioactivity counting cell. High flow-rates maintain the resolution achieved during the column separation at the expense of detector sensitivity, since the residence time of radioactive sample components in the counting cell is reduced at higher flows. Low eluent flows improve detector sensitivity, since the counting time is increased, but reduce chromatographic resolution owing to the increased turbulent mixing of the eluent in the measuring cell. The final compromise between component resolution and sensitivity is determined by the specific application and is dependent on whether sensitivity or resolution is the most important factor.

The effect of total gas flow through the gas proportional counter on detector sensitivity and component resolution is shown in Table 1. As the total flow through the counter was increased, the residence time decreased causing a reduction in detector sensitivity whilst improving resolution of the radio-peak. For example, with a total flow of 60 ml/min through the counting tube the integral of the chromatographed [1-^{14}C]hexadecane standard (in the plateau region of the response curve – see Section 3.2) was approximately 1920 counts. When the total flow was increased to 130 ml/min the integral of the injected standard decreased to approximately 510 counts owing to the lower residence time of the sample in the counting tube. The radio-peak width, w_{RAD}, at this flow was 16.9 s and was significantly less than that of 23.1 s measured with a flow of 60 ml/min. In both cases the w_{RAD} is increased, relative to the FID peak width, w_{FID}, by more than the residence time of the gas in the counting tube [11]. The additional peak broadening is primarily due to the large dead-volume introduced into the system by the oxidation furnace and the drying tube. These are the main areas where gas mixing occurs and chromatographic performance is lost.

In the radio-HPLC system the mass and radio-detectors were arranged in series hence the eluent flow-rate through both detectors was the same. The width of both mass (w_{UV}) and radio-peaks (w_{RAD}) reflects this since the broadening of the radio-peak relative to the mass peak is smaller than that observed with radio-GC (Table 2). The broadening that has taken place is most likely to have occurred in the radioactivity measuring cell. The effect of the increased flow-rate on the detector sensitivity can also be seen. The registered number of counts at a flow of 1 ml/min is approximately double that at 2 ml/min.

3.2. Effect of the scintillant/He-carrier gas composition on radioactivity measurement in the radio-GC gas proportional counter

The sensitivity of radioactivity detection in radio-GC is dependent on a combination of several factors.

Table 2
Effect of mobile phase flow-rate on peak width and detector sensitivity in radio-HPLC

Total flow (ml/min)	w_{UV} (s)	w_{RAD} (s)	Residence time (s)	[9-^{14}C]Fluorene radio-peak integral
1	36	48.2	9	24 999
2	18.3	28	4.5	12 720

The total gas flow-rate through the counting tube is one variable. A second variable is the composition of the mixture of carrier and scintillant gases in the counting tube. The latter affects both the plateau characteristics of the counting tube and the background count rate. Experiments were undertaken to determine the optimum ratio of carrier to scintillant gas through the gas-proportional counter with respect to the plateau characteristics of the counting tube and the background count rate. Both were evaluated by introducing a known amount of radioactive sample ([^{14}C]hexadecane dissolved in toluene) into the radio-GC system with the outlet splitter fully closed to direct the entire sample through the radio-detector. The flow of helium carrier and make-up gas was fixed at ≈30 ml/min whilst the scintillant gas flow was varied between 30 and 100 ml/min in four separate experiments. The ratio of He carrier gas flow to scintillant flow in the counting tube was found to influence markedly the counting efficiency of the detector. In particular, the voltage range over which the counter operated in the plateau region was extended with increasing scintillant gas content. This is in agreement with the work of Akira and Baba [12]. These workers investigated the impact of carrier–scintillant gas composition on the response of a gas proportional counter in a synchronised accumulating radioisotope detection (SARD) system. The final conditions employed a scintillant–helium-carrier gas ratio of 2:1 (50 ml/min Ar–CH_4 and 26 ml/min He) and an operating voltage of 1650 V. These conditions offered the best compromise in terms of sensitivity, background count rate and resolution of the radio-peaks. The plateau characteristics of the counting tube with this gas composition are illustrated in Fig. 1.

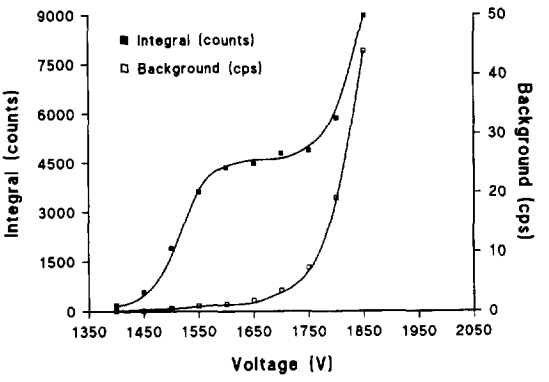

Fig. 1. Variation in radio-GC counting tube reponse with voltage at the chosen scintillant–carrier gas composition (Ar–CH_4:He, 2:1).

3.3. Radioactivity quantification using radio-GC

In order to achieve simultaneous radioactivity and mass measurement in radio-GC it is necessary to split the GC eluent between the mass and radio-detectors. This has imposed difficulties on the use of radio-GC for radioactivity quantification owing to the tendency for the split ratio to vary during temperature programmed analysis. Initial work employed a split ratio of 10:1 to ensure sufficient radioactivity was directed to the counting tube to be above the instrumental limits of detection. This was a primary concern since the specific activity of the exhaust samples was low owing firstly to the low rates of survival of the radiolabelled precursor (less than 1% of the radioactivity introduced into the engine survived combustion) and secondly to the dilution of radioactive components in the exhaust by their non-radiolabelled equivalents from the fuel. With an eluent split of 10:1 however, a five-fold increase in the split ratio was observed during the temperature programme. Variations in split ratio were determined by measuring the carrier gas flow to the FID system and to the radio-detector with the GC operated isocratically at a range of temperatures.

When the initial split ratio was reduced to 2.5:1 (at 40°C), a much smaller increase was observed during the temperature gradient (Fig. 2a). This ratio was

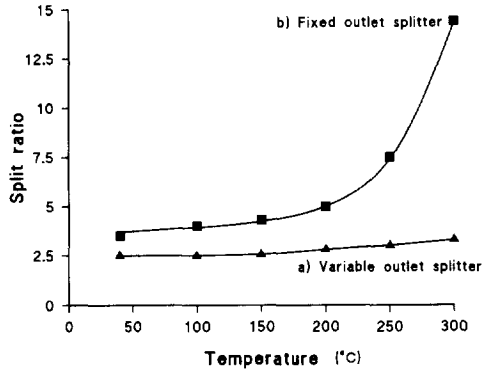

Fig. 2. Comparison of the variation in GC eluent split ratio with temperature for the variable and fixed outlet splitters.

found to direct sufficient sample to the radio-detector for identification and quantification purposes for the majority of exhaust samples. Mass measurement in radio-GC was not a problem since the mass of sample directed to the FID system was sufficient to enable measurement at most split ratios. The variation in split ratio may be due to variations in the rate of expansion of the components of the eluent splitter, which already partially obstructs the exit to FID and which has the effect of creating greater back-pressures at the exit to FID at higher split ratios (e.g. 10:1).

The variation in the eluent split, measured over a number of analyses, was found to be reproducible and was used to calibrate the instrument software to automatically compensate for changes in the split ratio in quantitative calculations. The system was evaluated by repeat analyses of [^{14}C]PAHs [naphthalene, fluorene, pyrene, and B(*a*)P] of known activity and eluting at a wide range of temperatures [≈120°C for naphthalene and ≈300°C for B(*a*)P] in a series of separate experiments. In each case, the calculated radioactivity showed less than ±10% error compared to the amount of radioactivity injected on-column (Table 3).

We attempted to split the GC eluent using an all glass three-way splitter with the length and diameter of the outlet pieces of deactivated silica tubing chosen to produce the required split ratio (10:1). However, a much greater increase in split ratio with temperature was observed with this system (Fig. 2b). The variation was caused by an increase in the viscosity of the carrier gas as the temperature increased. The greater volume of gas contained in the section of silica tubing connecting the splitter to the FID system generated a greater back-pressure than that created by the smaller volume of gas contained in the shorter length of silica tubing connecting the splitter with the radioactivity monitor. Rodriguez et al. [13] overcame the problem of the effect of temperature on the split ratio by installing the splitter in the heated detector manifold of the gas chromatograph.

3.4. Counting efficiency

The counting efficiency of the radioactivity monitor is a function of several parameters (Eq. 1):

$$\epsilon = \frac{CF_t}{sAV_d} \quad (1)$$

where ε=counting efficiency, s=split ratio (0–1.0), A=actual radioactivity of injected substance (dpm), V_d=volume of radioactivity detector (ml), F_t=total gas flow through detector (ml/min) and C=measured radioactivity of injected substance (counts).

The counting efficiency of radio-GC and radio-HPLC (in reversed-phase mode) detectors was determined by a series of repeat injections of [1-^{14}C]hexadecane and [9-^{14}C]fluorene, respectively. The counting efficiency of radio-GC, at the specified analysis conditions, was ca. 100% and is in agreement with radio-GC counting efficiencies quoted in the literature by other workers which ranged from 70 to 100% [13–15]. The variation in radio-HPLC counting efficiency with mobile phase composition was investigated by separate isocratic analyses with the eluent composition changed in separate analysis from 40 to 100% acetonitrile in water. The reduction in the measured radioactivity of the [^{14}C]B(*a*)P radio-peak compared with the known amount of radioactivity injected onto the column was the counting efficiency of the radioactivity monitor when operated in the reversed-phase mode and varied from

Table 3
Variation between applied and quantified radioactivity in radio-GC

PAH	Elution temperature (°C)	Applied radioactivity (Bq)	Quantified radioactivity (Bq)	Variation (%)
Naphthalene	120	620	595±26	4.2
Fluorene	165	450	480±35	7.8
Pyrene	245	380	402±18	4.7
Benzo[*a*]pyrene	300	540	535±10	1.9

65% with acetonitrile–water (40:60) to 68% with 100% acetonitrile.

3.5. Detector linearity and limits of detection

Limits of detection (LODs) for both GC and HPLC radioactivity monitors were taken as 3× signal-to-noise ratio (*S/N*). The noise level was determined by a series of blank analyses. Background values for the GC and HPLC radioactivity detectors at the specified analysis conditions were 48 cpm and 72 cpm, respectively. This produced detection limits for radio-GC of 3.2 Bq (1 Bq=1 disintegration per second) with an eluent split of 2.5:1, and 3.6 Bq for radio-HPLC (assuming a counting efficiency of 65%). In practice, several times this amount of radioactivity was required for quantification especially for radio-HPLC where broader radio-peaks make the task of identifying very low levels of radioactivity more difficult. These detection limits are in general agreement with those quoted by others working with flow-through GC and HPLC radioactivity monitors [13–15].

Radio-GC has slightly lower limits of detection than radio-HPLC and a higher counting efficiency, but suffers from the disadvantage of a lower sample loading capacity. A high sample loading capacity was essential to enable sufficient radioactivity to be introduced into the system to be above the analytical limits of detection of radio-GC. The megabore column allowed increased sample masses to be introduced into GC compared to capillary columns whilst achieving comparable resolution. The maximum sample loading capacity of the megabore column was 50 μg. Sample loading above this mass was found to affect the chromatographic performance of the system. Megabore columns are chosen for radio-GC work where the specific activity of samples is low [16].The linearity of response of the radio-detectors was investigated. [1-^{14}C]Hexadecane and [9-^{14}C]fluorene with activities ranging from 10 to 1000 Bq were introduced into radio-GC and radio-HPLC. The response of both detectors was linear over this range (R^2 = 0.996 and 0.998, respectively). The upper limit of this range more than encompasses the amount of radioactivity normally recovered in experimental situations.

3.6. Comparison of radio-GC and radio-HPLC

The techniques of radio-HPLC and radio-GC used in this research are complementary, with each technique offering advantages in different analytical situations. The benefits of radio-GC are primarily related to the greater resolving power of the system. The composition of the aromatic fraction of diesel exhaust is very similar to that of diesel fuel [17]. Both contain several major unsubstituted PAHs but alkylated PAHs (predominantly methyl and ethyl derivatives) comprise the bulk of aromatic species in both the fuel and emissions. Experiments in this laboratory have investigated the fate of alkyl PAHs during combustion since these species are major diesel fuel constituents and may have a significant effect on the composition of diesel exhaust emissions. Virtually all of the possible alkyl PAH isomers are present in diesel fuel (and hence in the emissions) and it is essential, when investigating their behaviour during diesel combustion, that the analytical technique be able to resolve the isomers sufficiently well to enable positive identification to be made. A large number of alkyl-PAH isomers have been conclusively identified by GC analysis from retention index data [18–20].

We have recently investigated the fate of [8-^{14}C]2-methylnaphthalene during diesel combustion. The radio-GC analysis of the naphthalene subsample of the exhaust is shown in Fig. 3. The major radio-peak (22 min 52 s, Fig. 3a) was identified as [^{14}C]2-methylnaphthalene, which had survived combustion (0.54%), by comparison of its retention time with that of the mass peak for 2-methylnaphthalene from the FID trace (22 min 41s, Fig. 3b). The time delay between the two detectors (11 s) was determined previously using [1-^{14}C]hexadecane standards. The small radio-peak (19.46 min) eluting prior to the main 2-methylnaphthalene radio-peak was identified as [8-^{14}C]naphthalene produced by the demethylation of [^{14}C]2-methylnaphthalene during combustion [21]. It can be seen from Fig. 3b that the 1-and 2-methylnaphthalene isomers were fully resolved which enabled conclusive assignment of the radio-peak identities. The peak eluting between the 1- and 2-methylnaphthalene isomers (Fig. 3b) is deuterated 2-methylnaphthalene added to the exhaust sample as an internal standard.

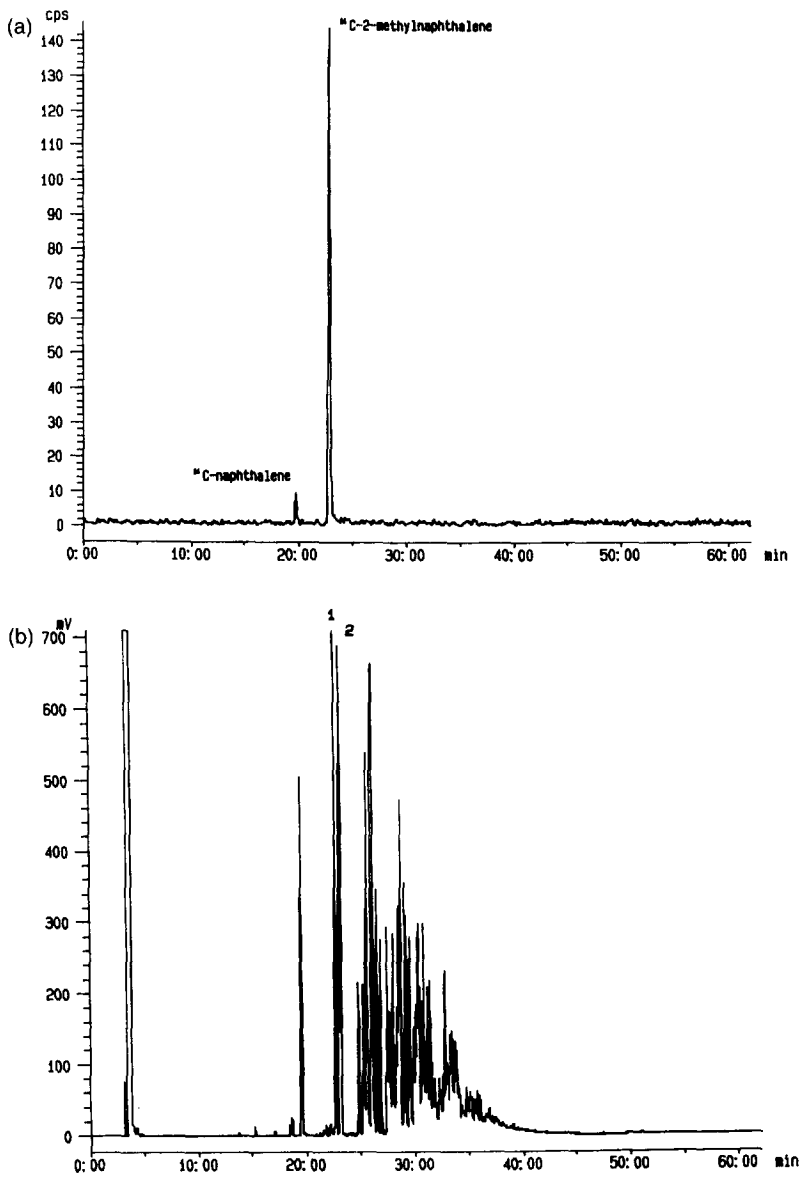

Fig. 3. Radio-GC analysis of naphthalene exhaust subsample from the combustion of [8-^{14}C]2-methylnaphthalene. (a) Radioactivity chromatogram and (b) FID chromatogram. Analysis conditions: DB-5 megabore column (30 m × 0.53 mm I.D.); temperature gradient, 40°C raised linearly to 300°C at 5°C/min; FID. Initial eluent split at 40°C = 2.5:1. Radio-detector conditions: scintillant gas flow, 50 ml/min; helium carrier flow, 26 ml/min; high voltage, 1650 V. Key: 1 = 2-methylnaphthalene; 2 = 1-methylnaphthalene.

The same subsample was also analyzed using reversed-phase radio-HPLC (Fig. 4). The order of elution of the 1- and 2-methylnaphthalene isomers in the HPLC separation is reversed with the 2-isomer eluting second (Fig. 4b). The UV and radio-detectors were connected in series. This gives rise to the slight time delay (≈15s) between the radio-peak and the mass peak of the [^{14}C]2-methylnaphthalene. It can be seen from Fig. 4 that the HPLC method has almost achieved a baseline separation of the two isomers. Assignment of the radio-peak identity is therefore as conclusive as in radio-GC analyses.

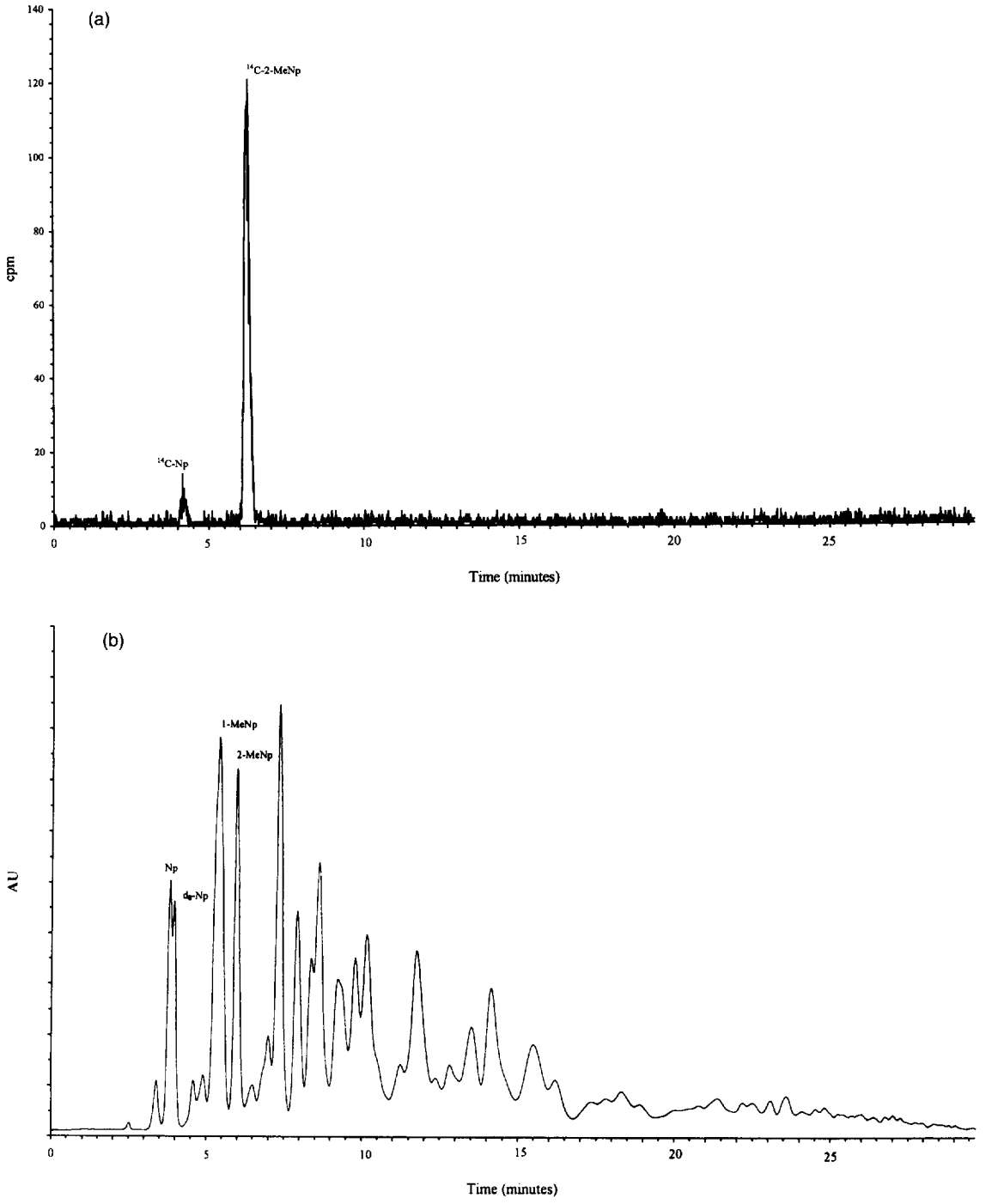

Fig. 4. Radio-HPLC analysis of naphthalene exhaust subsample from the combustion of [8-^{14}C]2-methylnaphthalene. (a) Radioactivity chromatogram and (b) UV chromatogram. Analysis conditions: Supelcosil LC-PAH column (250 × 4.6 mm I.D., 5 μm); solvent gradient, acetonitrile–water (60:40) for 5 min changed linearly to 100% acetonitrile over 20 min and held. Flow rate, 1 ml/min. UV detection at 254 nm.

However, the separation of di- and trimethylnaphthalenes isomers eluting later in the programme is poor when compared with the separation achieved using radio-GC. The challenge of identifying [^{14}C]alkyl-PAHs becomes more difficult as the number of possible isomers increases (e.g. trimethylnaphthalenes). Radio-GC is expected to be more useful in these analyses.

Radio-GC is also the preferred method of analysis in combustion experiments in which ^{14}C-labelled *n*-alkanes are used as radiotracers. Straight-chain alkanes are major diesel fuel components and are the

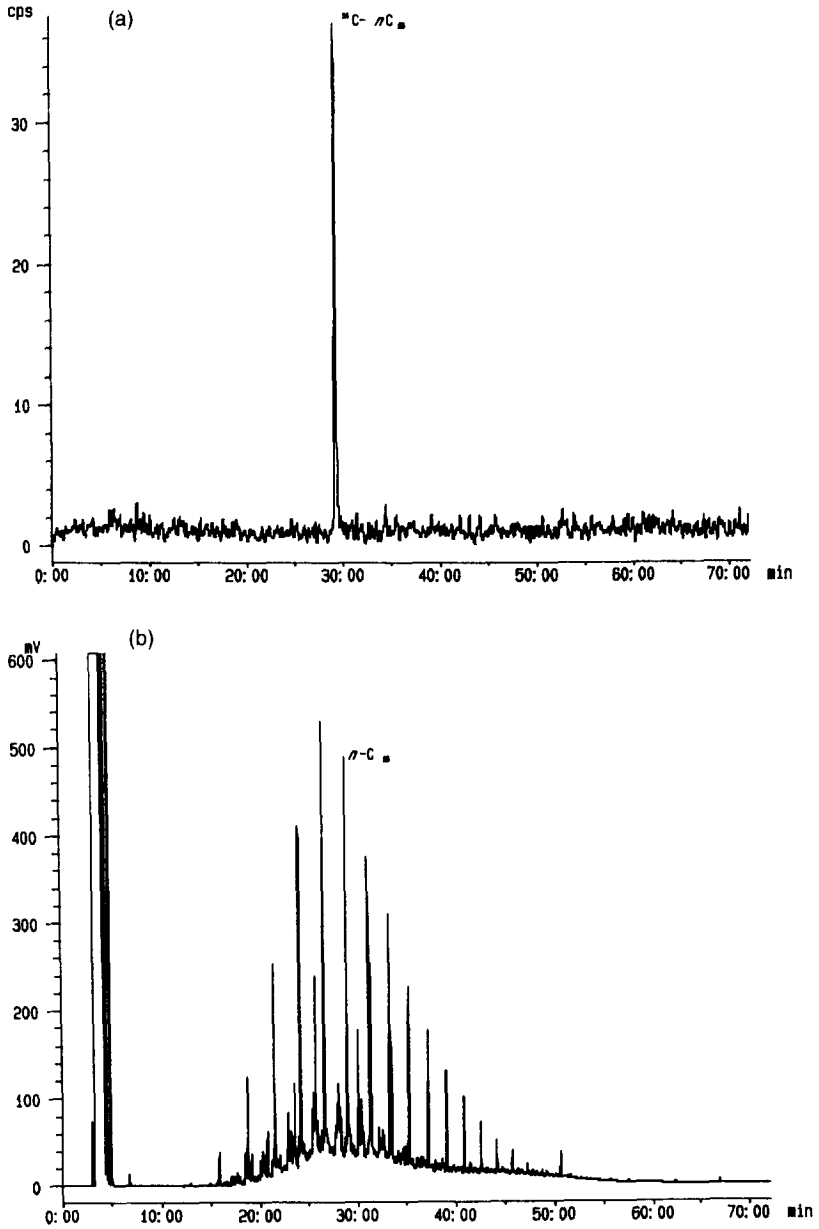

Fig. 5. Radio-GC analysis of aliphatic fraction of diesel exhaust from the combustion of [1-^{14}C]hexadecane. (a) Radioactivity chromatogram and (b) FID chromatogram. Analysis conditions as in Fig. 3.

major hydrocarbon species in the organic fraction of diesel exhaust emissions. These species are almost impossible to separate efficiently using other techniques. GC is ideally suited to the analysis of these compounds and they are separated according to their volatility. Fig. 5 illustrates the analysis of the aliphatic fraction of diesel exhaust collected from fuel spiked with [1-^{14}C]*n*-hexadecane (^{14}C-*n*C$_{16}$). The single radio-peak (29 min 11 s) was identified by comparison with standards as ^{14}C-*n*-C$_{16}$ surviving combustion (0.35%). The specific activity of the exhaust sample was lower than that of the [^{14}C]PAH exhaust subsamples since no additional fractionation is performed to concentrate radiolabelled aliphatic exhaust components. Pre-fractionation procedures for the separation of *n*-alkanes according to size may be performed using gel-permeation chromatography [22] and may be required in future work where the

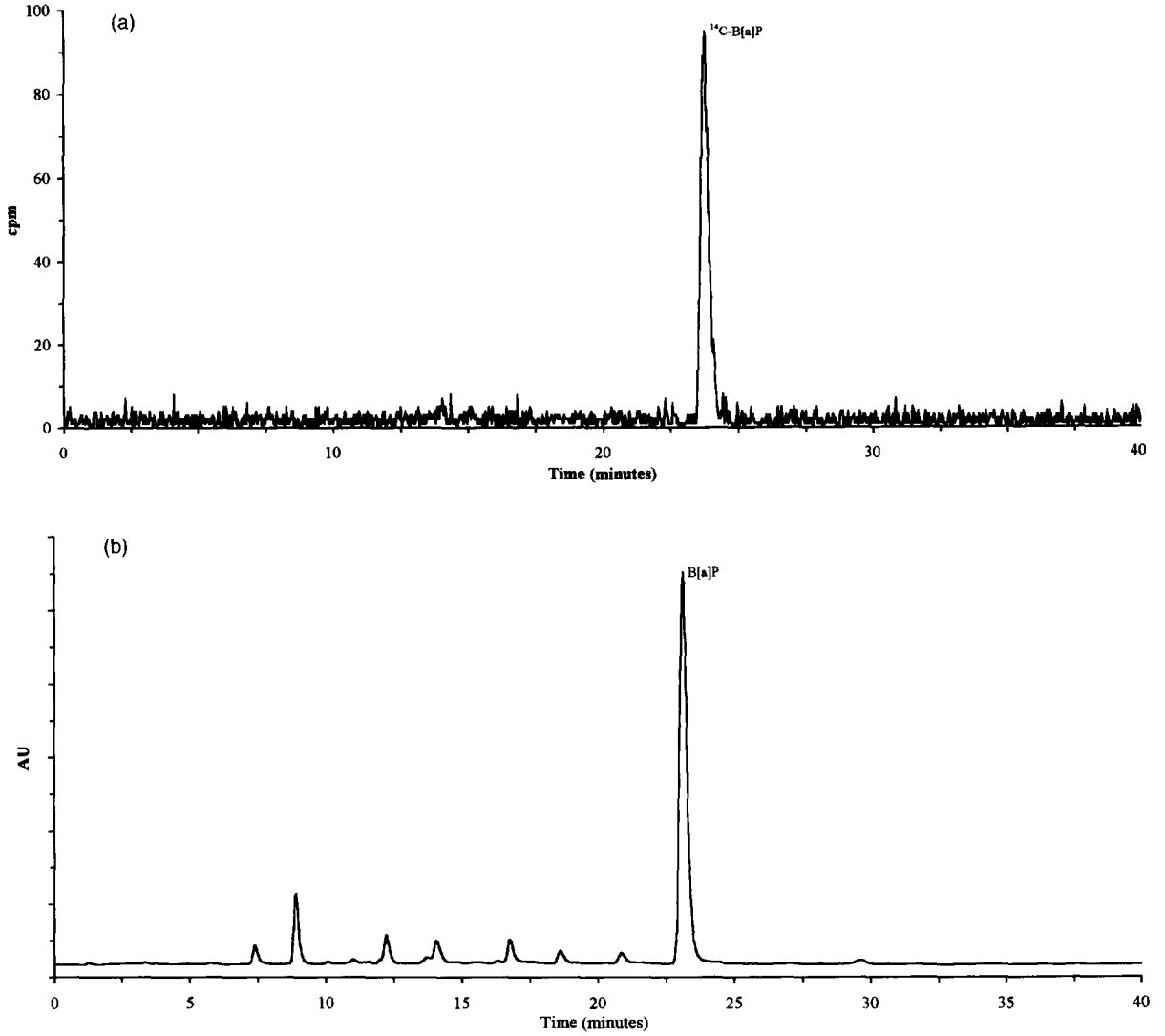

Fig. 6. Radio-HPLC analysis of 4- and 5-ring aromatic subsample of diesel exhaust from the combustion of [7,10-^{14}C]B(*a*)P [4]. (a) Radioactivity chromatogram and (b) fluorescence chromatogram. Analysis conditions: Supelcosil ODS LC-PAH column (250 × 4.6 mm I.D., 5 μm); solvent gradient, acetonitrile–water (80:20) changed linearly to 100% acetonitrile over 20 min and held for 20 min. Flow rate, 1 ml/min. Fluorescence detection, λ_{em} = 430 nm and λ_{ex} = 365 nm.

specific activity of radiolabelled aliphatic exhaust components is reduced.

Diesel emissions of certain organic components are extremely low, owing either to a low concentration in the fuel or a greater susceptibility for oxidation in the combustion chamber [4]. Benzo[*a*]pyrene survives the combustion process in very small quantities since it is comparatively reactive [6]. In our experiments, only 0.04% of the original [7,10-^{14}C]B(*a*)P radioactivity introduced into the engine survived combustion. Detection of ^{14}C-B(*a*)P in the emissions using radio-GC proved impossible despite the fractionation and concentration procedures employed in the analytical work-up. The higher loading capacity of analytical reversed-phase radio-HPLC has however enabled the [^{14}C]B(*a*)P to be detected and identified in the exhaust (Fig. 6).

4. Conclusions

This paper has described the novel application of radio-chromatographic techniques to the field of diesel emissions research. The techniques have demonstrated their suitability for this research showing both high sensitivity which has enabled low level radioactive products to be detected, and good resolution which has enabled conclusive identifications of radioactive products of combustion in the exhaust emissions.

Acknowledgments

This work was supported by the Engineering and Physical Sciences Research Council. The authors gratefully acknowledge the help provided by Mr. David Saunders of Unilever Research, Sharnbrook, Bedford.

References

[1] Diesel Vehicle Emissions and Urban Air Quality. Second Report of the Quality of Urban Air Review Group (QUARG), London, December, 1993.
[2] IARC Monographs, World Health Organization, Evaluation of Carcinogenic Risks to Humans: Diesel and Gasoline Engine Exhausts and Some Nitroarines, International Agency for Research on Cancer, Lyon, France, 1989.
[3] Society of Motor Manufacturers and Traders LTD, Statistical Department, Motor Industry of Great Britain, World Automotive Statistics, London, 1993.
[4] P.J. Tancell, M.M. Rhead, C.J. Trier, M.A. Bell and D.E. Fussey, Sci. Tot. Environ., 162 (1995) 179.
[5] G.S. Petch, C.J. Trier, M.M. Rhead, D.E. Fussey and G.E. Millward, Proc. Inst. Mech. Eng., 97 (1987) C340/87.
[6] P.J. Tancell, M.M. Rhead, R.D. Pemberton and J. Braven, Env. Sci. Technol., 29 (1995) 2871.
[7] W. Karcher, R.J. Fordham, J.J. Dubois, P.G.J.M. Glaude and J.A.M. Ligthart (Editors), Spectral Atlas of Polycyclic Aromatic Compounds, Vol. I, Reidel, Dordrecht, 1983.
[8] W. Jennings, Analytical Gas Chromatography, Academic Press, Ch. 5, 1987.
[9] D. Schuetzle, Env. Health Perspect., 47 (1983) 65.
[10] S.A. Wise, L.C. Sander and W.E. May, J. Chromatogr., 642 (1993) 329.
[11] M. Matucha, Chromatographia, 27 (1989) 552.
[12] K. Akira and S. Baba, J. Chromatogr., 489 (1989) 255.
[13] A. Rodriguez, C.R. Culbertson and C.L. Eddy, J. Chromatogr., 264 (1983) 393.
[14] L.A. Ernst, G.T. Emmons, J.D. Naworal and I.M. Campbell, Anal. Chem., 53 (1981) 1959.
[15] S. Baba, K. Akira, Y. Sasaki and T. Furuta, J. Chromatogr., 382 (1986)31.
[16] K. Akira and S. Baba, J. Chromatogr., 490 (1989) 21.
[17] P.T. Williams, M.K. Abbass and G.E. Andrews, Combust. Flame., 75 (1989)1.
[18] R. Alexander, R.I. Kagi and P.N. Sheppard, J. Chromatogr., 267 (1983) 367.
[19] S.J. Rowland, R. Alexander and R.I. Kagi, J. Chromatogr., 294 (1984) 407.
[20] D.L. Vassilaros, R.C. Kong, D.W. Later and M.L. Lee, J. Chromatogr., 252 (1982) 1.
[21] M.M. Rhead and R.D. Pemberton, in preparation.
[22] B.A. Bidlingmeyer and F.V. Warren, LC·GC, 6 (1988) 780.